(9) J. W. McIver, *J. Am. Chem. Soc.*, **94**, 4782 (1972).
(10) J. W. McIver, *Acc. Chem. Res.*, **7**, 72 (1974); *J. Am. Chem. Soc.*, **97**, 3632 (1975).
(11) M. J. S. Dewar, A. C. Griffin, and S. Kirschner, *J. Am. Chem. Soc.*, **96**, 6225 (1974).
(12) A. Komornicki, unpublished work in our laboratories.
(13) L. A. Burke, G. Leroy, and M. Sana, *Theor. Chim. Acta*, **40**, 313 (1975).
(14) R. E. Townshend, G. Ramunni, G. Segal, W. J. Hehre, and L. Salem, *J. Am. Chem. Soc.*, **98**, 2190 (1976).
(15) Cf. M. J. S. Dewar, G. P. Ford, and H. S. Rzepa, *Chem. Commun.*, 728 (1977).
(16) L. A. Burke and G. Leroy, *Theor. Chim. Acta*, **44**, 219 (1977).
(17) D. Poppinger, *J. Am. Chem. Soc.*, **97**, 7486 (1975).
(18) The MNDO RHF surface for the reaction of **4** and **5** is qualitatively similar to that reported here for the reaction of **1** and **2** and different from the one reported by Poppinger.[17] The MNDO transition state for **4** + **5** has the structure a, with a calculated activation energy of 26 kcal/mol. This transition state leads to the formation of a stable zwitterionic intermediate (no negative eigenvalues in the Hessian matrix) b and passage over a further barrier (structure c) with an activation energy of only 0.8 kcal/mol leads to the product isoxazole. The structure and energy reported by Houk et al.[22] refer to structure c and *not* the true transition state for the reaction a.

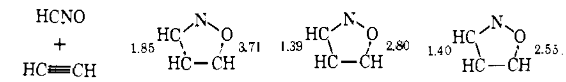

a b c

ΔH_f = 108.1 kcal/mol ΔH_f = 133.9 kcal/mol ΔH_f = 111.0 kcal/mol ΔH_f = 111.8 kcal/mol

(19) D. Poppinger, *Aust. J. Chem.*, **29**, 465 (1976).
(20) (a) J. W. McIver and A. Komornicki, *Chem. Phys. Lett.*, **10**, 303 (1971); (b) J. W. McIver and A. Komornicki, *J. Am. Chem. Soc.*, **94**, 2625 (1972); (c) D. Poppinger, *Chem. Phys. Lett.*, **35**, 550 (1975).
(21) M. V. Basilevsky, A. K. G. Shamov, and V. A. Tikhomirov, *J. Am. Chem. Soc.*, **99**, 1369 (1977).
(22) P. Caramella, K. N. Houk, and L. N. Domelsmith, *J. Am. Chem. Soc.*, **99**, 4514 (1977).
(23) A. W. Salotto and L. Burnelle, *J. Chem. Phys.*, **52**, 2936 (1970).
(24) M. J. S. Dewar, S. Olivella, and H. S. Rzepa, *Chem. Phys. Lett.*, **47**, 80 (1977).
(25) P. A. Cox and M. H. Wood, *Theor. Chim. Acta*, **41**, 269, 279 (1976).
(26) M. J. S. Dewar and C. E. Doubleday, *J. Am. Chem. Soc.*, submitted for publication.
(27) For example, the difference in the energies obtained using a 2 × 2 CI based on closed shell orbitals, and a 3 × 3 CI based on open shell orbitals was less than 3 kcal/mol for all the systems studied here.
(28) For "normal" closed shell molecules, the single configuration MINDO/3, UMINDO/3, and MINDO/3-CI all gave very similar energies (see Table I).
(29) M. J. S. Dewar and G. P. Ford, *J. Am. Chem. Soc.*, **99**, 7822 (1977).
(30) M. J. S. Dewar and H. S. Rzepe, *J. Mol. Struct.*, **40**, 145 (1977).
(31) M. J. S. Dewar and G. P. Ford, *J. Am. Chem. Soc.*, **99**, 8343 (1977).
(32) M. J. S. Dewar and A. Komornicki, *J. Am. Chem. Soc.*, **99**, 6174 (1977).
(33) See C. J. Collins and N. S. Bowman, *ACS Monogr.*, **No. 167** (1970).
(34) J. A. Barnard and J. K. Parrott, *J. Chem. Soc., Faraday Trans. 1*, 2404 (1976). In this, and other[35] work, a value for E_a of 67 kcal/mol was obtained. Our analysis of the ir data gave $\Delta H^\ddagger$ 65 kcal/mol, which is consistent with the difference of RT between E_a and $\Delta H^\ddagger$.
(35) M. Uchiyama, T. Tomioka, and A. Amano, *J. Phys. Chem.*, **68**, 1878 (1964).
(36) Cf. studies of rotational barriers in ethylenes, allenes, and butadienes, unpublished work in these laboratories.
(37) (a) E. Clementi, *J. Chem. Phys.*, **38**, 2248 (1964); (b) *ibid.*, **39**, 487 (1964).
(38) D. Rowley and H. Steiner, *Discuss. Faraday Soc.*, **10**, 198 (1951), reported measurements which gave E_a(800 K) = 27.5 kcal/mol, from which they calculated E_a(0 K) = 25.1 kcal/mol. Townshend et al.[14] calculated a value for $\Delta H^\ddagger_0$ of 34.3 kcal/mol, based on ΔH°_0 for **2** + **3** → **1** and the activation energy for the reverse reaction (E_a = 66.7 kcal/mol) reported previously.[34,35] The best estimate for $\Delta H^\ddagger_{298}$ is probably 27–34 kcal/mol.
(39) An alternative, and complementary, criterion is to inspect either the value of $\langle S^2 \rangle$ given by the UMINDO/3 method or the eigenvectors of the CI matrix when using CI. Biradicaloids normally have values for $\langle S^2 \rangle$ which are greater than 1.0 or have nearly equal contributions from the two closed shell configurations a^2 and b^2 (see Table I).
(40) See J. B. Lambert, C. D. McLaughlin, and V. Mark, *Tetrahedron*, **32**, 2075 (1976), for a particularly elegant demonstration of the stereospecificity of the Diels-Alder reaction of perchlorocyclopentadiene and α-methylstyrene.
(41) M. B. Epstein, K. S. Pitzer, and F. D. Rossini, *J. Res. Natl. Bur. Stand.*, **42**, 379 (1949).
(42) See C. W. Bauschlicher, Jr., K. Haber, H. F. Schaefer, III, and C. F. Bender, *J. Am. Chem. Soc.*, **99**, 3610 (1977), and papers cited there.
(43) See M. J. S. Dewar, G. P. Ford, M. L. McKee, H. S. Rzepa, and L. E. Wade, *J. Am. Chem. Soc.*, **99**, 5069 (1977).
(44) A. Sauer, H. Wiest, and A. Mielert, *Chem. Ber.*, **97**, 3183 (1964).
(45) D. Rowley and H. Steiner, *Discuss. Faraday Soc.*, **10**, 198 (1951).
(46) This assumption is supported by several investigations that seem to indicate that butadiene and its methyl derivatives react at similar rates with dienophiles; see, e.g., R. A. Fairclough and C. N. Hinshelwood, *J. Chem. Soc.*, 236 (1938). The difference in rate between butadiene and cyclopentadiene probably corresponds to the heat of isomerization of the former into the cis conformation needed for the reaction.
(47) O. Diels and U. Alder, *Ann. Chem.*, **460**, 19 (1928); **470**, 68 (1929).
(48) See M. J. S. Dewar and R. C. Dougherty, "The PMO Theory of Organic Chemistry", Plenum Press, New York, N.Y., 1975, p 316.
(49) M. J. S. Dewar, *J. Am. Chem. Soc.*, **74**, 3350 (1952).
(50) M. J. S. Dewar, T. Mole, and E. W. T. Warford, *J. Am. Chem. Soc.*, 3581, (1956).
(51) M. J. S. Dewar, *J. Am. Chem. Soc.*, **74**, 3357 (1952).
(52) G. B. Kistiakowsky and W. Ransom, *J. Chem. Phys.*, **7**, 725 (1939).
(53) A. Wasserman, *J. Chem. Soc.*, 612 (1942).

The Electronic States of Ni_2 and Ni_2^+

Thomas H. Upton and William A. Goddard III*

Contribution No. 5646 from the Arthur Amos Noyes Laboratory of Chemical Physics, California Institute of Technology, Pasadena, California 91125.
Received August 10, 1977

Abstract: Extensive generalized valence bond (GVB) and configuration interaction calculations (POL-CI) have been carried out for the lowest states of Ni_2 and Ni_2^+ for bond lengths from 1.6 to 4.0 Å. The six lowest states of Ni_2 are found to be essentially degenerate with an average equilibrium bond length R_e = 2.04 Å and D_e = 2.92 eV. A $^4\Sigma_u^-$ ground state is found for the ion with a bond length R_e = 1.96 Å and dissociation energy D_e = 4.14 eV. The bonding of Ni is dominated by the interactions of the 4s orbitals on each Ni with each Ni of Ni_2 corresponding to a $(4s)^1(3d)^9$ configuration. The lowest states lead to singly occupied δ orbitals on each center with other 3d occupations leading to 100 electronic states within about 1.0 eV of the ground state.

I. Introduction

The diatomic molecules formed of the first-row transition elements represent a potential source of information relevant to the study of organometallic complexes, surface chemistry, and solid-state physics. Unfortunately, isolation of these molecules from the bulk metal is very difficult to do in a manner that allows proper characterization. Experimental data to date on these molecules are scarce[1-3] and quite inconclusive.

Until recently, high-quality theoretical studies of these molecules were not feasible. With the development of sound effective potential techniques the size of the problem has been greatly reduced. As a first step toward calculations on larger clusters of Ni atoms, we have carried out a study of the bonding

0002-7863/78/1500-5659$01.00/0

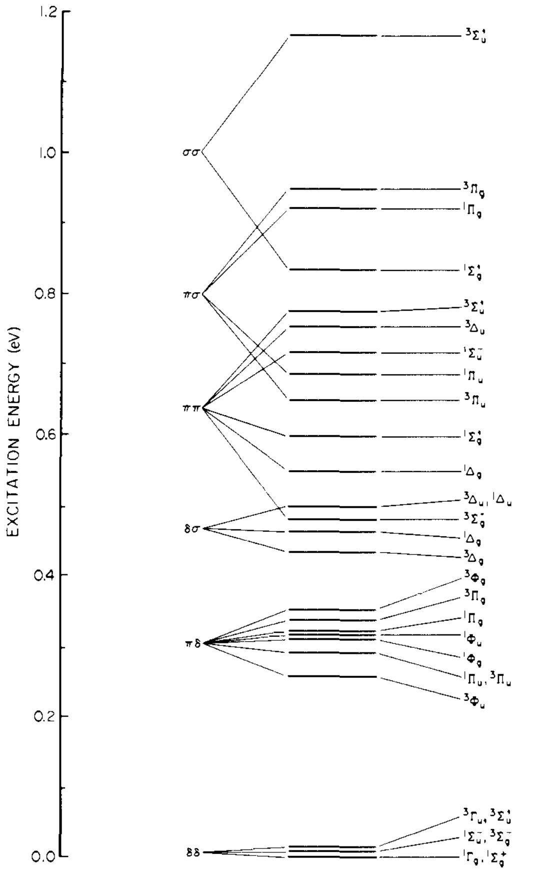

Figure 1. States of Ni_2 arising from possible occupations allowing a 3d hole on each center. 4s–4s bond exists for all states.

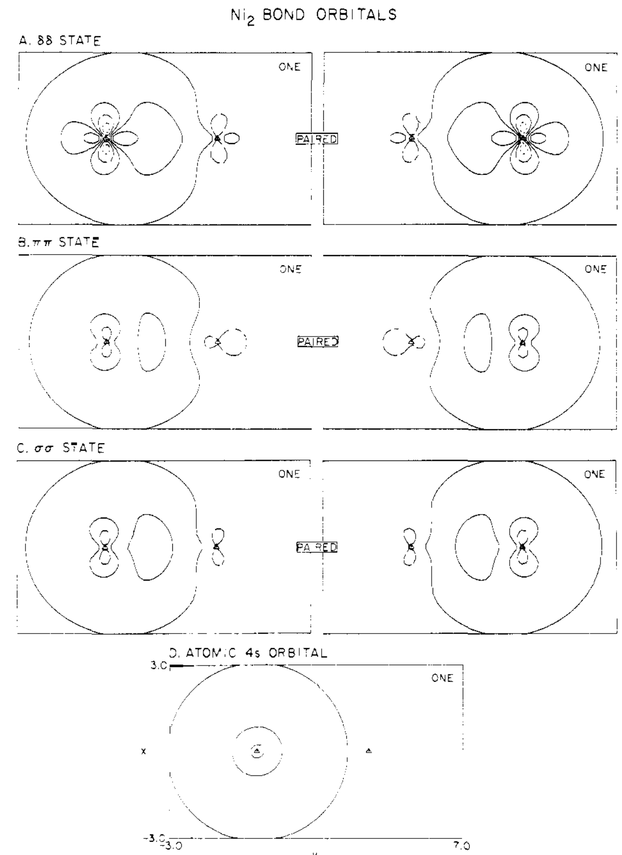

Figure 2. The bond orbitals for several states of Ni_2. Note the hybridization and polarization of the orbital for the δδ state. The atomic 4s orbital is shown for reference. Long dashes indicate nodal lines.

in Ni_2 and Ni_2^+. In this paper we report the results of extensive generalized valence bond (GVB) and configuration interaction (CI) calculations on the lower states of these two molecules. In section II we present a basic qualitative description of the bonding of Ni_2 followed by a more thorough discussion of the details. In section III a similar treatment is given for Ni_2^+. Section IV describes the methods used, and in the final section (V) we relate our results to the known experimental data and discuss the implications on studies of larger clusters.

II. The Ni_2 Molecule

A. Qualitative Description. In this section we will develop a qualitative description of the states of Ni_2 by starting with the separated Ni atoms. The ground state of the Ni atom is $^3F_4$ corresponding to a configuration[4] $[Ar]4s^23d^8$, while the first excited state (0.03 eV above $^3F_4$) is the $^3D_3$ corresponding to a configuration of $[Ar]\,4s^13d^9$. On the other hand, averaging the J components of each state (corresponding approximately to ignoring spin–orbit coupling), the ground state is $^3D(s^1d^9)$ while the $^3F(s^2d^8)$ state is only 0.03 eV higher.

Consider now bringing together two Ni atoms in the $s^2d^8(^3F)$ state. The size of a 4s orbital is about twice that of a 3d orbital. This indicates that the interactions of two Ni atoms will be dominated by the 4s orbitals on each center. As a result, two s^2d^8 atoms will interact in a repulsive manner as they approach one another (analogous to He_2 or Be_2). Two $s^1d^9(^8D)$ atoms, however, each have half-filled 4s orbitals and can interact in a bonding manner as the orbitals begin to overlap (much as in H_2). Similarly, an s^2d^8 Ni atom coupled with an s^1d^9 Ni will lead to a total of three electrons in the 4s shell and would not be expected to bond as strongly as in the s^1d^9–s^1d^9 case. The basic picture then for the lower Ni_2 states will be of a single 4s bond, analogous to the alkali metals or H_2. This leaves a single uncoupled 3d electron on each center, leading to a possibility of $(5 \times 2 \times 5 \times 2) = 100$ states, depending on their spin coupling (75 triplets and 25 singlets) and orbital occupation. We will use a particle-hole notation in referring to the various states, where δδ, ππ, δπ, etc., define the specific holes in the 3d shell of each atom. In all cases for Ni_2, a 4s–4s σ bond is understood.

The spectrum of states that results for Ni_2 is shown qualitatively in Figure 1. The states may be grouped, as shown, by their hole designations. In terms of the coupling of two Ni atoms, the trends shown here imply that a δ hole is energetically most favorable, with π and σ holes significantly less so. This contradicts the ordering that is obtained by the application of simple ligand field or crystal field arguments (i.e., the splitting resulting from overlapping filled ligand orbitals). As discussed elsewhere,[5] the origin for this ordering of states may be found in the configuration mixing that occurs upon hybridizing the 4sσ bond. In hybridizing this orbital to form the bond, each $4s^13d^9$ Ni mixes a component of $4s^23d^8$ Ni. The 3d occupation on the s^1d^9 Ni determines which components of s^2d^8 will be used. A ^3D Ni with a δ hole will mix in a low-lying s^2d^8 configuration with δσ holes. A π hole in the ^3D atom forces the mixing of a higher πσ hole s^2d^8 atom, while a σ hole in the ^3D forces mixing of very high-lying σσ hole s^2d^8 components. As a first approximation, these interactions are responsible for the ordering shown in Figure 1. The σ bond pairs for the σσ, δδ, and ππ states of Ni_2 are shown in Figure 2 (along with a 4s atomic orbital for reference). The δδ hole state may be seen to have much greater $3d_{z^2}$ character in its 4s pair than either the ππ or σσ states. This mixing is the only essential difference between these states and seems to be responsible for the slightly stronger bond in the δδ hole states. We will consider each of the possible hole combinations more carefully below.

B. Detailed Discussion of d–d Interactions. 1. σ–σ States.

The σ–σ states have a singly occupied d_σ orbital on each Ni. These can be coupled into singlet and triplet states, ${}^1\Sigma_g^+$ and ${}^3\Sigma_u^+$. Ignoring the 4s–4s bond (which is common to both states), ${}^1\Sigma_g^+$ can be considered as having a $3d\sigma$–$3d\sigma$ bond while ${}^3\Sigma_u^+$ has a $3d\sigma$–$3d\sigma$ antibond. Thus these states are analogous to the corresponding 1s–1s states of H_2. The difference is that at R_e for H_2 the 1s–1s overlap is ~0.8 leading to a ${}^3\Sigma_u^+$–${}^1\Sigma_g^+$ separation of 10 eV, while for Ni_2 the $d\sigma$–$d\sigma$ overlap is ~0.07 leading to a ${}^3\Sigma_u^+$–${}^1\Sigma_g^+$ separation of 0.33 eV (at $3.8a_0$). Thus, although the ${}^1\Sigma_g^+$ state of Ni_2 can be formally represented as Ni=Ni with 4s–4s and $3d\sigma$–$3d\sigma$ bonds, the $3d\sigma$–$3d\sigma$ overlap is too small for a real bond. The $3d_{z^2}$ and 4s overlaps for the ${}^1\Sigma_g^+$ state are plotted as a function of bond length in Figure 3. For comparison, the overlaps of atomic orbitals are shown as well.

2. δ–δ States. States of this type will have doubly occupied $3d_\sigma$ orbitals on each Ni. An examination of Figure 4, where potential curves for $\delta\delta$ and $\sigma\sigma$ states are shown, indicates that the effect of these extra electrons is to increase slightly the bond length as well as to increase the harmonic force constant for the $\delta\delta$ (${}^1\Sigma_g^+$) state. These changes are a result of the fact that any overlap of the $3d_{z^2}$ orbitals now leads to repulsive interactions between the two centers. Unlike the $\sigma\sigma$ hole states, there is a number of states arising from $\delta\delta$ holes, differing only in the manner that the singly occupied δ orbitals are coupled. Looking only at the δ orbitals, a single Ni atom will be depicted as

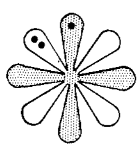

where the set of shaded lobes represent one of the δ's (δ_1 or $\delta_{x^2-y^2}$) and the unshaded lobes the other δ (δ_2 or δ_{xy}). Thus defined, the possible ways in which two Ni atoms may be coupled are shown below where the dots indicate how many electrons are in each orbital:

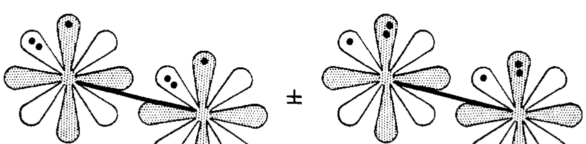

(1a)
(1b)

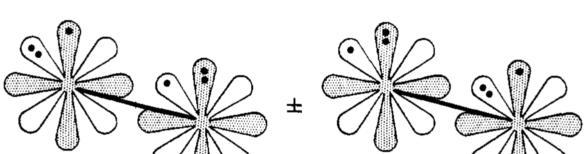

(2a)
(2b)

The four $\delta\delta$ configurations have been grouped so as to indicate the resonant and antiresonant combinations. The symmetries resulting from these combinations are

$${}^3\Sigma_u^+,\ {}^1\Sigma_g^+ \quad (+\text{ sign}) \quad (1a)$$
$${}^3\Gamma_u^+,\ {}^1\Gamma_g^+ \quad (-\text{ sign}) \quad (1b)$$
$${}^3\Sigma_g^-,\ {}^1\Gamma_g^- \quad (+\text{ sign}) \quad (2a)$$
$${}^3\Gamma_u^-,\ {}^1\Sigma_u^- \quad (-\text{ sign}) \quad (2b)$$

For (1a) and (1b), two singly occupied orbitals can singlet couple to form a weak δ bond, the singlet necessarily lower than the triplet. For (2a) and (2b) the singly occupied orbitals are orthogonal. With either configuration alone, the triplet would be expected to be lower by twice the exchange integral:

$$(\delta_{1\ell}\delta_{2r}|\delta_{2r}\delta_{1\ell})$$

For the bond lengths of interest in Ni_2, this exchange integral is very small, ranging from 6.6×10^{-5} hartree at 3.0 bohr to 3×10^{-6} hartree at 7.5 bohr. For such a small exchange integral, the two spin states are expected to be essentially degenerate throughout the bonding region of the potential curve. When varying the bond length through distances ranging from R_e to very large R, as has been done here, it is not adequate to consider only one spin coupling. The correct wave function for the ground state must possess the capability of going to the separated atom limit to produce two ${}^3D$ Ni atoms, each with the 4s electron high-spin coupled to the $3d_\delta$ orbital. The overlap between the two δ orbitals is small enough that the coupling of the two triplets is determined almost completely by the 4s orbitals. At larger R this necessarily leads to the singlet being lower.

In order to compare (1) with (2), it is necessary to consider the doubly occupied δ orbitals. For the configurations shown in (1), a weak δ_1 bond is formed, but there are doubly occupied δ_2 orbitals on each center that lead to repulsive interactions. For the configurations in (2) a doubly occupied orbital interacts with a singly occupied orbital, allowing the doubly occupied orbital to delocalize slightly on to the other center. The singly occupied orbital must become orthogonal and takes on antibonding character. Orbitals optimized to describe one of the configurations in (2) with singlet-coupled δ orbitals are shown in Figure 5. (Only the $\delta_{x^2-y^2}$ orbitals are shown, the δ_{xy} orbitals being equivalent to these.) Here it can be seen that the delocalization of the doubly occupied δ is so slight that the only indication of its occurrence is the node built in by the singly occupied orbital for orthogonality. The net bonding interaction

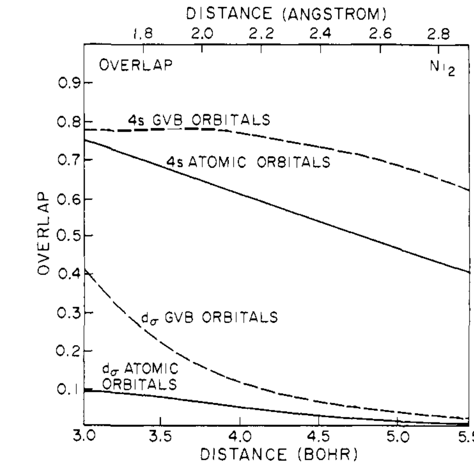

Figure 3. Overlap of 4s and $3d_{z^2}$ atomic orbitals as a function of R. Also shown are the overlaps from GVB calculations on the ${}^1\Sigma_g^+$ state.

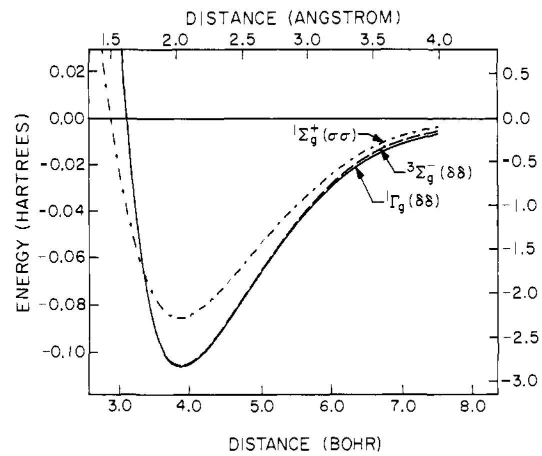

Figure 4. Potential curves for several states of Ni_2 (from POL–CI calculations).

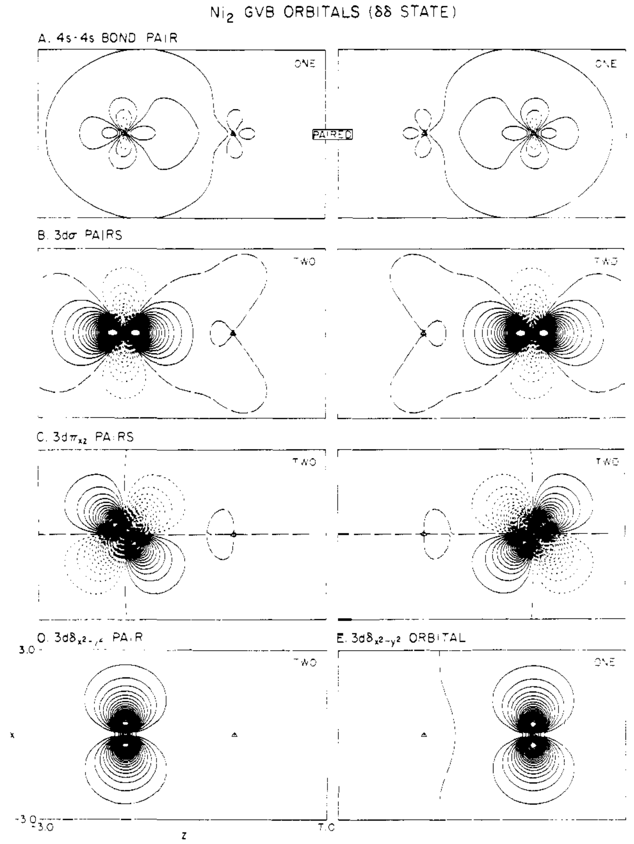

Figure 5. Contour plots of Ni_2 orbitals obtained from GVB calculations corresponding to one of the configurations in (2). The $3d\pi_{yz}$ and $3d\delta_{xy}$ orbitals are omitted. Long dashes indicate nodal lines.

here, however small, should be more important than bonding occurring in (1), leading to (2) being slightly lower than (1). It is unlikely that these effects will be large. As a result, the splitting of states similar to (1) and (2) remains very small, with singlets in each case being slightly lower than the triplets. Resonance stabilization of (1) or (2) is virtually nonexistent.

C. Intermediate States. A similar type of analysis may be applied to those states occurring intermediate in energy to the $\delta\delta$ and $\sigma\sigma$ states. As in the $\delta\delta$ case, all of the states in this region may be taken as resonant and antiresonant combinations of equivalent VB configurations (which themselves do not possess full molecular symmetry).

There are eight states with $\pi\pi$ holes that are completely analogous to (1) and (2). Here again, a doubly occupied $3d_\pi$ orbital may overlap a singly occupied orbital on the opposite center as in (2) for the $\delta\delta$ case, and this type of state is expected to be the lowest in energy. Using the notation of (1) and (2), where now the orbitals are $3d_\pi$ (but with the same resonance combinations), the resulting states are

$$^3\Sigma_u^+,\ ^1\Sigma_g^+ \quad (+\text{ sign}) \qquad (1a')$$

$$^3\Delta_u^+,\ ^1\Delta_g^+ \quad (-\text{ sign}) \qquad (1b')$$

$$^3\Sigma_g^-,\ ^1\Delta_g^- \quad (+\text{ sign}) \qquad (2a')$$

$$^3\Delta_u^-,\ ^1\Sigma_u^- \quad (-\text{ sign}) \qquad (2b')$$

The overlap of the π orbitals on each center is not as small as in the $\delta\delta$ case. This leads to a noticeable resonance stabilization energy whose effect may be seen by examining Figure 1. There is a much greater separation between $\pi\pi$ resonant and antiresonant states (e.g., $^1\Delta_g$ and $^1\Sigma_u^-$ or $^1\Delta_g$ and $^1\Sigma_g^+$) than there is between analogous $\delta\delta$ hole states. The exchange integral

$$(\pi_{xz\ell}\pi_{yzr}|\pi_{yzr}\pi_{xz\ell})$$

is no longer insignificant (it is 0.002 hartree = 0.05 eV) at R_e, causing $^3\Sigma_g^-$ to drop below the $^1\Delta_g$, in opposition to what occurs for the $\delta\delta$ hole states.

The $\pi\delta$ states present a slightly different problem. Here there are eight equivalent VB configurations which may be denoted as (singly occupied orbitals only)

$$\delta_{1\ell}\pi_{xzr},\ \delta_{1\ell}\pi_{yzr},\ \delta_{2\ell}\pi_{xzr},\ \delta_{2\ell}\pi_{yzr} \qquad (3a)$$

$$\delta_{1r}\pi_{xz\ell},\ \delta_{1r}\pi_{yz\ell},\ \delta_{2r}\pi_{xz\ell},\ \delta_{2r}\pi_{yz\ell} \qquad (3b)$$

where subscripts ℓ and r refer to left and right, and each term represents an antisymmetrized pair. Owing to the equivalence of π_{xz} and π_{yz} holes, as well as δ_1 and δ_2 holes, proper resonance is obtained only upon combination of four of these configurations as follows:[6]

$$\mathcal{A}[(\delta_{1\ell}\pi_{xzr} + \delta_{1r}\pi_{xz\ell}) \pm (\delta_{2\ell}\pi_{yzr} + \delta_{2r}\pi_{yz\ell})] \quad \begin{cases} ^{3,1}\Pi_g^+ \ (+\text{ sign}) & (4a) \\ ^{3,1}\Phi_g^+ \ (-\text{ sign}) & (4b) \end{cases}$$

$$\mathcal{A}[(\delta_{1\ell}\pi_{xzr} - \delta_{1r}\pi_{xz\ell}) \pm (\delta_{2\ell}\pi_{yzr} - \delta_{2r}\pi_{yz\ell})] \quad \begin{cases} ^{3,1}\Pi_u^+ \ (+\text{ sign}) & (5a) \\ ^{3,1}\Phi_u^+ \ (-\text{ sign}) & (5b) \end{cases}$$

$$\mathcal{A}[(\delta_{1\ell}\pi_{yzr} + \delta_{1r}\pi_{yz\ell}) \pm (\delta_{2\ell}\pi_{xzr} + \delta_{2r}\pi_{xz\ell})] \quad \begin{cases} ^{3,1}\Phi_g^- \ (+\text{ sign}) & (6a) \\ ^{3,1}\Pi_g^- \ (-\text{ sign}) & (6b) \end{cases}$$

$$\mathcal{A}[(\delta_{1\ell}\pi_{yzr} - \delta_{1r}\delta_{yz\ell}) \pm (\delta_{2\ell}\pi_{xzr} - \delta_{2r}\pi_{xz\ell})] \quad \begin{cases} ^{3,1}\Phi_u^- \ (+\text{ sign}) & (7a) \\ ^{3,1}\Pi_u^- \ (-\text{ sign}) & (7b) \end{cases}$$

This leads to eight covalent states for singlet and triplet, which may be viewed as having two types of resonance occurring simultaneously. For both singlets and triplets, the stabilization resulting from *left-right* resonance (terms in parentheses, e.g., $\delta_{1\ell}\pi_{xzr} \pm \delta_{1r}\pi_{xz\ell}$) is more important than resonance between orbitals on the same centers (between *pairs* of parentheses, e.g., $\delta_{1\ell}\pi_{xzr} \pm \delta_{2\ell}\pi_{yzr}$). This can be seen by examination of Figure 1.

Finally, there are $\delta\sigma$ and $\pi\sigma$ hole states. As expected, all of the $\delta\sigma$ states lie beneath the $\pi\sigma$ states in energy. There are four covalent Δ states with $\delta\sigma$ holes that separate in energy roughly into two pairs. These pairs consist of resonant ($^{1,3}\Delta_g$) and antiresonant ($^{1,3}\Delta_u$) combinations of form

$$\mathcal{A}(\delta_\ell\sigma_r \pm \sigma_\ell\delta_r) \qquad (8)$$

The splitting energy is about 0.05 eV and is due to the overlap of σ orbitals in the resonance configurations. Similar states are obtained for $\pi\sigma$ holes. The overlap between π orbitals is six times that of the δ orbitals at R_e; thus the split between resonant ($^{1,3}\Pi_u$) and antiresonant ($^{1,3}\Pi_g$) states is about 0.25 eV here.

III. The Ni_2^+ Ion

A. Qualitative Description. As in the case of neutral Ni_2, we will begin by first examining the possible couplings at very long R. The ground state for the ion is ^2D with configuration $4s^03d^9$ which lies 7.62 eV above the ground state of Ni.[4] The first excited state for Ni^+ is ^4F which is 1.08 eV above the ^2D state and has the configuration $4s^13d^8$. The separated atom limit for Ni_2^+ is expected to be one of the following couplings ($Ni-Ni^+$)

$^3D-^2D$	$^3F-^2D$	$^3D-^4F$	$^3F-^4F$
($s^1d^9-s^0d^9$)	($s^2d^8-s^0d^9$)	($s^1d^9-s^1d^8$)	($s^2d^8-s^1d^9$)
0.0 eV	0.03 eV	1.08 eV	1.11 eV
($s^1d\sigma^4$)	($s^2d\sigma^3$)	($s^2d\sigma^3$)	($s^3d\sigma^2$)

where the σ shell occupation is given in parentheses below the energy value (ionization is assumed to occur from the σ shell[7]). The importance of a strong 4s bond in the lower states of Ni_2 has been demonstrated and the same reasoning should apply here. As is the case for Ni_2, s^2d^8–s^1d^9 coupling involving three 4s electrons should be less advantageous. The s^1d^9–s^0d^8 coupling leads to a one-electron 4s bond and is reasonably strong. For example, the positive ion formed from each of the diatomic alkali metals involves essentially a one-electron ns bond, and each is more tightly bound than the corresponding neutral.[8] A similar ordering (bond energy ion > bond energy neutral) has been observed for each of the first-row transition metal diatomics.[2] This coupling, as well as the $s^2d\sigma^3$ couplings (which are found to lead to the ground state), will be examined in more detail.

B. Detailed Description of Bonding. In Figure 6, the spectrum of states for Ni_2^+ is shown for a bond length of 3.8 bohr. Two sets of states are shown, corresponding to those having an $s^2d\sigma^n$ σ shell (Figure 6a) and those that have an $s^1d\sigma^{n+1}$ σ shell (Figure 6b). The preference for particular types of holes is exhibited in a similar manner as for Ni_2. The situation is somewhat complicated now as it is possible for the s^1 and s^2 states of the same symmetry to mix, leading to stabilized and destabilized mixtures. As an example we will consider the $\delta\delta$ hole states. For Ni_2 both $^3\Sigma_g^-$ and $^1\Sigma_u^-$ $\delta\delta$ states occur low in energy. Removing a 3d electron from the $^3\Sigma_g^-$ leads to possible $^{4,2}\Sigma_u^-$ s^2 states. Removing a 4s electron from the $^1\Sigma_u^-$ state produces a $^2\Sigma_u^-$ s^1 state. These $^2\Sigma_u^-$ states will mix, leading to the low-lying $\delta\delta$ state of this symmetry shown in Figure 6b. This mixing occurs very strongly in the Ni_2^+ states making it difficult in some cases to unambiguously assign them as s^1 or s^2. These states are marked with an asterisk in Figure 6. In still other cases it was not possible to assign even the occupation character, and these have been left unassigned in the figure.

A more notable difference that appears between Ni_2 and Ni_2^+ is that the low-spin coupling of the $\delta\delta$ holes does not lead to the ground state. The explanation for this lies in the two-electron energy terms. Evaluating the two-electron energy for the three-electron, three open-shell quartet (ignoring closed shells)

$$\varphi_1 = \mathcal{A}\{\delta_{1\ell}\delta_{2r}\sigma_\ell(\alpha\alpha\alpha)\} \tag{9}$$

leads to the two-electron terms

$$E_{\varphi_1} = J_{\delta_{1\ell}\delta_{2r}} - K_{\delta_{1\ell}\delta_{2r}} + J_{\delta_{1\ell}\sigma_\ell} - K_{\delta_{1\ell}\sigma_\ell} + J_{\delta_{2r}\sigma_\ell} - K_{\delta_{2r}\sigma_\ell}$$

where

$$J_{ij} = (ii|jj) \geq 0$$
$$K_{ij} = (ij|ij) \geq 0$$

There are two doublets possible given by

$$\varphi_2 = \mathcal{A}\{\delta_{1\ell}\delta_{2r}\sigma_\ell(\alpha\beta - \beta\alpha)\alpha\} \tag{10}$$

$$\varphi_3 = \mathcal{A}\{\delta_{1\ell}\delta_{2r}\sigma_\ell(2\alpha\alpha\beta - \alpha\beta\alpha - \beta\alpha\alpha)\} \tag{11}$$

These lead to the two-electron energies

$$E_{\varphi_2} = J_{\delta_{1\ell}\delta_{2r}} + K_{\delta_{1\ell}\delta_{2r}} + J_{\delta_{1\ell}\sigma_\ell} + J_{\delta_{2r}\sigma_\ell} - \tfrac{1}{2}(K_{\delta_{1\ell}\sigma_\ell} + K_{\delta_{2r}\sigma_\ell})$$

$$E_{\varphi_3} = J_{\delta_{1\ell}\delta_{2r}} - K_{\delta_{1\ell}\delta_{2r}} + J_{\delta_{1\ell}\sigma_\ell} + J_{\delta_{2r}\sigma_\ell} + \tfrac{1}{2}(K_{\delta_{1\ell}\sigma_\ell} + K_{\delta_{2r}\sigma_\ell})$$

Combining,

$$E_{\varphi_1} - E_{\varphi_2} = -2K_{\delta_{1\ell}\delta_{2r}} - \tfrac{1}{2}(K_{\delta_{1\ell}\sigma_\ell} + K_{\delta_{2r}\sigma_\ell})$$
$$E_{\varphi_1} - E_{\varphi_3} = -\tfrac{3}{2}(K_{\delta_{1\ell}\sigma_\ell} + K_{\delta_{2r}\sigma_\ell})$$

It has been shown previously that $K_{\delta_{1\ell}\delta_{2r}}$ is very small; however, the remaining exchange integrals are not, and they are responsible for the observed preference for the high-spin coupling. The other effects observed, which lead to splittings of the various states (e.g., resonance, electron–electron repulsion, etc.) in Ni_2, apply identically to Ni_2^+.

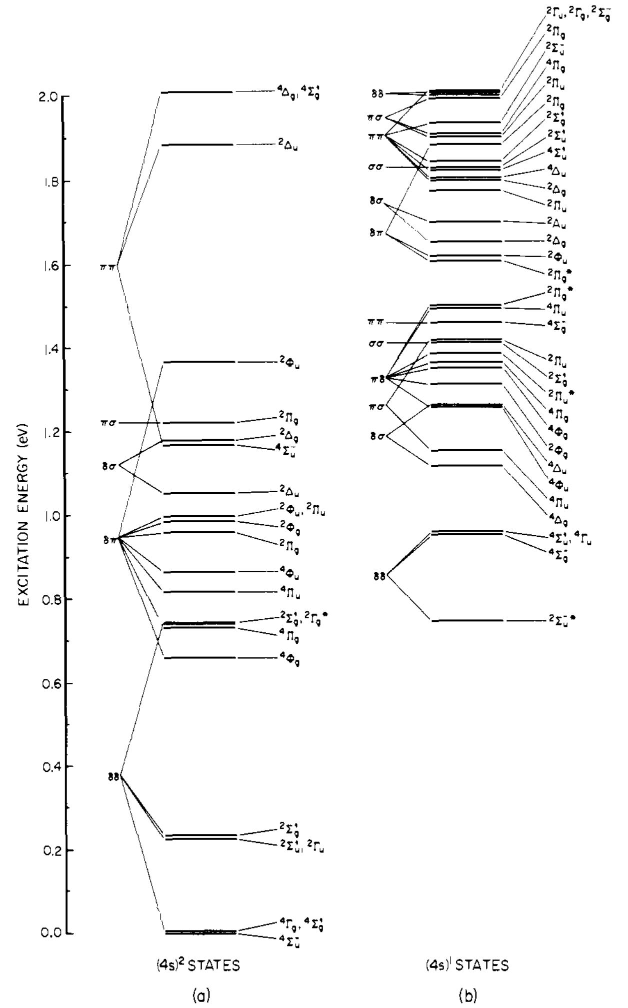

Figure 6. States of Ni_2^+ arising from possible location of 3d holes on each center. Ionization from 4s ($4s^1$) or $3d\sigma(4s^2)$ orbitals was allowed, giving rise to the two sets of states shown. Not all assignments are unambiguous; those shown with an asterisk are questionable.

From Figure 6, it can be seen that the preference for the $s^2d\sigma^3$ σ shell over the $s^1d\sigma^4$ is not great; at R = 3.8 au, the $\delta\delta$ states resulting from each are separated by less than 1 eV. As is explained in more detail in Appendix I, the relative importance of either of these couplings is a function of bond length and is given by the approximate terms:

$$E_2^x = \frac{2S\tau}{1+S^2} \qquad E_1^x = \frac{\tau}{1+S}$$

where E_2^x and E_1^x represent the exchange effects responsible for bonding in the two- and one-electron bonds, respectively. The quantity τ is the *one-electron* contribution

$$\tau = h_{\ell r} - \tfrac{1}{2}S(h_{\ell\ell} + h_{rr})$$

The point of such a partitioning of the energy terms is to make clear the dependence of the bonding energy on the degree of overlap between centers. When S is small, $E_1^x \ll E_2^x$, leading to $s^1d\sigma^4$ states being lower than analogous $s^2d\sigma^3$ states. However, as S increases with decreasing R, a crossing point is reached and the two-electron bond may become lower. These points may be seen more clearly by examining Figure 7. The $^2\Sigma_g^+$ and $^4\Sigma_g^-$ states shown are $s^1d\sigma^2$ and $s^1d\sigma^4$ states, respectively. The crossing occurs in the region of 5 bohr, and for all

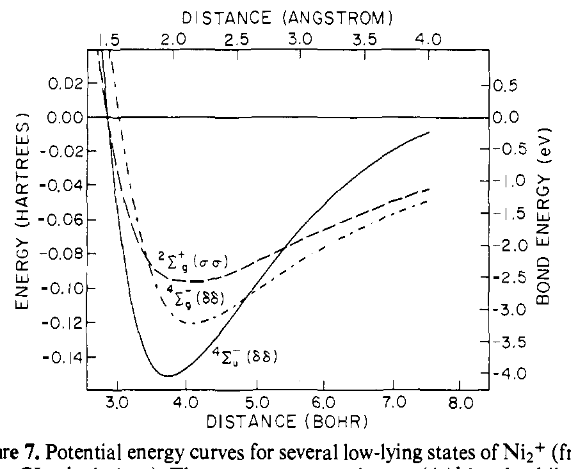

Figure 7. Potential energy curves for several low-lying states of Ni_2^+ (from POL-CI calculations). The two upper states have a $(4s)^1$ bond, while the lowest state has a $(4s)^2$ occupation.

larger R, the $s^1d\sigma^{n+1}$ states are lower in energy. For the same reasons, the minima for both $^2\Sigma_g^+$ and $^4\Sigma_g^-$ occur at longer bond lengths than the $^4\Sigma_u^-$ state.

There are other factors which may lead to an ever greater preference for the s^2d^3 states than is indicated above. There are two separate couplings of Ni and Ni^+, both of which lead to σ occupation. By the noncrossing rule, the ground state must dissociate into the lowest of these, a s^2d^8 (^3F) Ni and a s^0d^9 (^2D) Ni^+. In Figure 8 the orbitals for a quartet $\delta\delta$ hole state are shown. Qualitatively, the shapes of the π and δ orbitals are very similar to those shown for the $\delta\delta$ singlet coupled state of Ni_2. The σ shell has altered greatly owing to the loss of the $3d_{z^2}$ electron. The double occupied $3d_{z^2}$ has delocalized slightly onto the other center forcing the $3d_{z^2}$ orbital there to take on antibonding character to remain orthogonal. The 4s orbital on the left has shifted away from the double occupied orbital. For the orbitals shown here, there is a net charge on the left of −0.34. Clearly this does not possess proper symmetry, and a rather complicated set of equivalent δ, $3d_\sigma$, and 4s resonance configurations are required in the actual wave function. There will be two ways to describe the σ resonance corresponding to the $s^2d^8(^3F)$-$s^0d^9(^2D)$ coupling of Ni-Ni^+

$$\mathcal{A}\{(\sigma_{\ell s}{}^2 \pm \sigma_{rs}{}^2)(\alpha\beta - \beta\alpha)(\sigma_{\ell d}{}^2\sigma_{rd} \pm \sigma_{rd}{}^2\sigma_{\ell a})(\alpha\beta - \beta\alpha)\alpha\} \quad (12)$$

or the $s^1d^9(^3D)$-$s^1d^8(^4F)$ coupling of Ni-Ni^+

$$\mathcal{A}\{(\sigma_{\ell s}\sigma_{rs} + \sigma_{rs}\sigma_{\ell s})(\alpha\beta - \beta\alpha)(\sigma_{\ell d}{}^2\sigma_{rd} \pm \sigma_{rd}{}^2\sigma_{\ell d})(\alpha\beta - \beta\alpha)\alpha\} \quad (13)$$

The splitting in (12) will be large owing to the 4s-4s overlap; however, (13) shows no 4s resonance and should not have such widely separated resonant and antiresonant states. Careful examination of the 4s orbitals shown in Figure 8 indicates that the resonance there is not describable by either (12) or (13) above taken separately. The ground-state wave function is a stabilized mixture of both of these wave functions. This favorable mixing, along with the loss of a $3d_\sigma$ electron, is probably the reason that $^4\Sigma_u^-$ Ni_2^+ is more strongly bound at a shorter R_e than $^4\Sigma_g^-$ Ni_2^+ or $^1\Gamma_g(^3\Sigma_u^+)$ Ni_2.

IV. Calculational Details

A. Effective Potential and Basis Set. In all of the calculations reported here, we make use of the fact that the argon core for the first row transition elements is essentially noninteracting and thus replaceable by an effective potential. This reduces the SCF problem to one of optimizing only the valence orbitals. We first used the potential of Melius, Olafson, and Goddard[9] which was fit to an ab initio description of the Ni atom. This

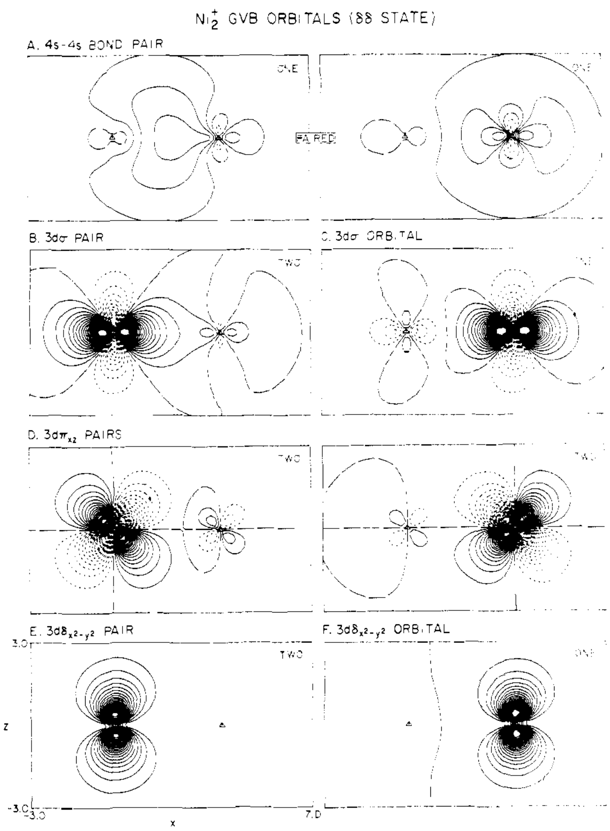

Figure 8. Contour plots of orbitals for Ni_2^+ obtained from GVB calculations for δ orbital occupation as in (2), and a $3d\sigma$ hole. Long dashes indicate nodal lines.

potential was modified by Sollenberger, Goddard, and Melius[10] to incorporate intraatomic electron correlation effects in an approximate sense, leading to the modified effective potential (MEP) used in all calculations reported here.

The basis set consisted of a (4s, 4p, 5d) set of Gaussians on each center. Of the five d functions from Wachters,[11] the inner four were contracted together using the atomic coefficients. By using the effective potential, it was only necessary to use the four most diffuse s functions from Wachters' set (the inner two were contracted together using coefficients from the ^3D atomic state). The p functions used were obtained by Sollenberger; the inner three were contracted together using coefficients from the atomic state. This scheme results in a (3s, 2p, 2d) set of contracted Gaussians on each center.

B. Wave Functions. The primary goals in these calculations were to obtain not only good binding energies but also a clear physical description of the orbital interactions as a function of bond length. Almost all of the lower states of Ni_2 and Ni_2^+ involve weakly overlapping singly occupied 3d orbitals. Thus, even at R_e, where the Hartree-Fock description is usually acceptable, many of the states cannot be properly described by this type of wave function. The GVB wave function, allowing each electron in a bonding pair to occupy its own orbital, accounts for the major correlation effects, leading to a qualitatively useful description. The separated atoms each possess at least four doubly occupied valence orbitals, allowing us to choose as a minimal description for the molecule a GVB wave function that includes eight doubly occupied orbitals and four singly occupied orbitals. We find that the two 4s orbitals are always coupled into a singlet GVB pair for Ni_2. The remaining two singly occupied orbitals have 3d character and allow the generation of all low-lying states. From these GVB calculations we obtain a set of spatially optimized orbitals (see Figures 5 and 8) from which we can obtain a good description of the bonding.

Table I. Equivalence of Configurations Based on Localized or Atomic Orbitals and Configurations Based on Delocalized Symmetry Functions

	localized										delocalized										
orbital	$\delta_{x^2-y^2}$		δ_{xy}			$\delta_{x^2-y^2}$		δ_{xy}			$\delta_{x^2-y^2}$		δ_{xy}			$\delta_{x^2-y^2}$		δ_{xy}			
function type	L	R	L	R		L	R	L	R		G	U	G	U		G	U	G	U		eq
configurations[a]	(2	1	1	2)	+	(1	2	2	1)		(2	1	2	1)	−	(1	2	1	2)		(2a)
	(2	1	1	2)	−	(1	2	2	1)		(1	2	2	1)	−	(2	1	1	2)		(2b)
	(2	2	1	1)	+	(1	1	2	2)		(2	2	1	1)	+	(1	1	2	2)		(1a)
	(2	2	1	1)	−	(1	1	2	2)		(2	2	1	1)	−	(1	1	2	2)		(1b)

[a] For example, (2 1 1 2) indicates configuration $\delta^2_{x^2-y^2a}\delta^1_{x^2-y^2b}\delta^1_{xya}\delta^2_{xyb}$.

The GVB wave function accounts for the important electron correlation effects, but does not possess $D_{\infty h}$ symmetry. Using these orbitals, however, we can perform small CI calculations that will build in resonance effects and provide the proper symmetry.

To make use of the full diatomic symmetry in these CI calculations, it is convenient to project the localized GVB orbitals into a set of symmetry orbitals. For a CI wave function, which includes resonance terms, the use of such functions is not a restriction. The equivalence of the localized and delocalized descriptions for this type of wave function is demonstrated for $\delta\delta$ hole cases in Table I. In making the transformation from localized to delocalized orbitals we have used the simple relations

$$\phi_g = (\phi_\ell + \phi_r)\frac{1}{\sqrt{2(1+S)}} \qquad \phi_u = (\phi_k - \phi_r)\frac{1}{\sqrt{2(1-S)}}$$

A similar analysis may be performed for each of the other combinations of holes.

For Ni_2, to obtain a basis for the CI, we begin with the set of 12 localized GVB orbitals corresponding to a triplet-coupled $\delta\delta$ hole state with occupation as in one of the configurations of (2a) or (2b). We form the symmetric and antisymmetric projections, then orthogonalize to obtain 12 valence and 12 virtual symmetry orbitals. The process of orthogonalization changes the character of the valence orbitals somewhat but use of the virtuals allows this to be corrected in the CI. For the states of Ni_2^+ an analogous procedure was followed. The GVB orbital set used as a basis was that shown in part in Figure 8.

C. GVB–CI. The spectrum of states for Ni_2 and Ni_2^+ shown qualitatively in Figures 1 and 6 was obtained from a small restricted CI designed to characterize the ordering of states. In doing such a small CI, the configurations necessary to describe different occupations of the same symmetry (e.g., $^3\Sigma_g^-$ which arises from $\delta\delta$ and $\pi\pi$ hole states) could be allowed to interact within a single calculation and many more states could be obtained inexpensively. It was found that such interactions were not important and that the states could be clearly assigned in most cases according to the scheme presented in sections II and III.

The method used to generate the configurations for the GVB–CI was straightforward. No excitations were allowed into the virtual orbitals. All $\sigma\rightarrow\sigma$, $\pi\rightarrow\pi$, $\delta\rightarrow\delta$ excitations were allowed but no excitations to shells of different ℓ values were allowed. The resulting set of configurations could be separated into symmetry types under D_{2h} and each type solved for separately.

The basis used for these calculations involved valence σ and δ orbitals obtained from a triplet-coupled $\delta\delta$ hole GVB calculation. The π basis was from an analogous $\pi\pi$ hole state. To avoid bias due to the different spatial character of singly and doubly occupied orbitals, the π and δ orbitals were averaged after projecting into symmetric and antisymmetric combinations.

D. POL–CI. This larger CI is designed to allow changes of orbital shape to occur when the full resonance is included in the wave function. Thus, in addition to excitations important for the GVB–CI, we allow single excitations into a set of virtual orbitals to allow "polarization" of the occupied orbitals. It was of obvious interest to fully examine the $^1\Gamma_g(\delta\delta)$ and $^3\Sigma_g^-(\delta\delta)$ states as they are nearly degenerate candidates for the ground state. We also chose to further examine the $^1\Sigma_g^+(\sigma\sigma)$ state since it initially seemed a clear choice for the ground state. More importantly, as a $\sigma\sigma$ hole state, it allows us to gauge the distance between the highest and lowest of the $4s^2$ states of Ni_2 as a function of bond length. For Ni_2^+ there were three states of primary interest. Aside from the $^4\Sigma_u^-(s^2d\sigma^3)$ ground state, it was of interest to carefully determine the applicability of the one-electron bond ideas to Ni_2^+; thus the $^4\Sigma_g^-(s^1d\sigma^4)$ state was considered. In the same manner as for Ni_2, it was of interest to examine the $^2\Sigma_g^+(\sigma\sigma)$ state (also a $4s^1$ state) to determine the full range of 3d occupation effects as a function of bond length.

The manner in which the configurations were obtained for this state may best be seen by examining a particular occupaion, for example, triplet-coupled $\delta\delta$ holes analogous to (2). The GVB wave function replaces the product

$$\mathcal{A}\{\varphi_{4s}\varphi_{4s}(\alpha\beta - \beta\alpha)\}$$

with the pair correlation function

$$\mathcal{A}\{(\phi_{4s\ell}\phi_{4sr} + \phi_{4sr}\phi_{4s\ell})\chi\}$$

where $\phi_{4s\ell}$ and ϕ_{4sr} are allowed to be completely general. In terms of symmetry orbitals, this becomes

$$\mathcal{A}\{(\phi_{4sg}^2 - \lambda^2\phi_{4su}^2)\chi\} \tag{14}$$

This leads to two configurations describing the correlation in the 4s orbital; combining these with the four resonance configurations described by Table I leads to eight of the configurations shown in Table IIA. (The remaining four involve the $4sg^14su^1$ occupation.) For the triplet-coupled $\delta\delta$ hole states of (1), the configurations are shown in Table IIB. From this basic set, all singles into the virtual orbitals were considered under the restriction that only $\sigma_{val}\rightarrow\sigma_{virt}$, $\pi_{val}\rightarrow\pi_{virt}$, and $\delta_{val}\rightarrow\delta_{virt}$ be allowed. The results of these POL–CI calculations for the lowest states of Ni_2 and Ni_2^+ are listed in Table III. In Table IV we compare the total energies for these states as obtained from each level of calculation reported here for a fixed bond distance of 2.01 Å.

V. Discussion

A. The Bond Length. The Ni–Ni bond length in the bulk metal is 2.49 Å,[12] as compared with our value for Ni_2 of 2.04 Å. Such short metal–metal distances are quite unusual, even for those binuclear complexes with metal–metal bonds.[13] This short distance finds some support, however, in the recent work of Efremov et al.[14] Their rotational analysis of a band characteristic of the Cr_2 dimer[15] indicates a bond length of 1.71 Å, which is consistent with the result reported here. Melius, Upton, and Goddard[16] have examined a cluster of 13 Ni atoms consisting of a central Ni and 12 neighbors as in the free metal. An optimization of the bond length for this cluster yielded an

Table II. Configuration Basis for the POL–CI Calculations

	$4s_g$	$4s_u$	$3d_{\sigma_g}$	$3d_{\sigma_u}$	π_{xzg}	π_{xzu}	π_{yzg}	π_{yzu}	$\delta_{x^2-y^2g}$	$\delta_{x^2-y^2u}$	δ_{xyg}	δ_{xyu}
	2	0	2	2	2	2	2	2	2	1	2	1
	2	0	2	2	2	2	2	2	1	2	1	2
	2	0	2	2	2	2	2	2	2	1	1	2
	2	0	2	2	2	2	2	2	1	2	2	1
	0	2	2	2	2	2	2	2	2	1	2	1
A	0	2	2	2	2	2	2	2	1	2	1	2
	0	2	2	2	2	2	2	2	2	1	1	2
	0	2	2	2	2	2	2	2	1	2	2	1
	1	1	2	2	2	2	2	2	2	1	2	1
	1	1	2	2	2	2	2	2	1	2	1	2
	1	1	2	2	2	2	2	2	2	1	1	2
	1	1	2	2	2	2	2	2	1	2	2	1
	2	0	2	2	2	2	2	2	2	2	1	1
	2	0	2	2	2	2	2	2	1	1	2	2
B	0	2	2	2	2	2	2	2	2	2	1	1
	0	2	2	2	2	2	2	2	1	1	2	2
	1	1	2	2	2	2	2	2	2	2	1	1
	1	1	2	2	2	2	2	2	1	1	2	2

Table III. POL–CI Results for Ni_2 and Ni_2^+

	state	R_e, Å	ω_e, cm^{-1}	D_e, eV
Ni_2	$^1\Sigma_g^+(\sigma\sigma)$	2.03	308.6	2.36
	$^3\Gamma_u(\delta\delta)$	2.05	346.5	2.91
	$^3\Sigma_u^+(\delta\delta)$	2.05	349.3	2.92
	$^1\Sigma_u^-(\delta\delta)$	2.04	347.1	2.92
	$^3\Sigma_g^-(\delta\delta)$	2.04	342.5	2.92
	$^1\Sigma_g^+(\delta\delta)$	2.04	344.8	2.93
	$^1\Gamma_g(\delta\delta)$	2.04	344.2	2.93
	exptl[a]			2.4
Ni_2^+	$^2\Sigma_g^+(\sigma\sigma)$	2.15	178.7	2.64
	$^4\Sigma_g^-(\delta\delta)$	2.16	303.0	3.31
	$^4\Sigma_u^-(\delta\delta)$	1.97	390.0	4.14
	exptl[a]			3.8

[a] Reference 1. In obtaining D_e values, Kant used estimates of R_e = 2.30 Å and ω_e = 325 cm^{-1}.

Ni–Ni distance of 2.41 Å, quite close to the value of 2.49 Å for Ni metal. Whereas two Ni atoms may interact strongly with one another, the implication here is that the presence of other neighboring atoms (or ligands in finite complexes) leads to additional repulsive interactions between nonbonded electron pairs forcing the larger bond length. Thus the large difference between the atomic radii for the bulk metal and the (calculated) bond length of the dimer appears to be real.

B. The $\delta\delta$ Ground State. The calculation of a $\delta\delta$ hole ground state finds support in similar calculations that have been carried out on the NiH molecule. Here the hydrogen atom bonds directly to the singly occupied Ni 4s orbital, leaving a single 3d hole on the Ni atom. It is found that the lowest state of this system is the $^2\Delta$ state which has a $3d_\delta$ hole.[10] In this case, experimental results clearly show a $^2\Delta_{5/2}$ ground state.[17]

C. The MO Description. It is important to note that a similar treatment of Ni_2 using molecular orbitals would lead to very different results. The difficulty is a result of the extremely small overlap ($S < 0.01$) that exists between dδ orbitals on different centers. Just as the MO wave function is far more successful at describing the lowest triplet state of H_2 than the lowest (ground state) singlet state at large separation, here a bias toward high-spin states is introduced in the MO description of Ni_2. In section IVD and Table I we have demonstrated the equivalence of the MO and VB in describing $\delta\delta$ hole triplet states. There is no corresponding set of resonance configurations that may be used for singlet $\delta\delta$ hole states. Electron correlation error, a problem for H_2 only at large separation, seriously affects Ni_2 singlet wave functions at equilibrium separation. Thus the $^1\Sigma_g^+$ ($\delta\delta$) state and $^1\Gamma_g^+$ component of the $^1\Gamma_g$ ($\delta\delta$) state are both found to be almost 10 eV higher in the MO description. Clearly, a vast expansion of Figure 4 would be required to include the same spectrum of states described by MO wave functions. Only those singlet states resulting from the open-shell coupling of singly occupied orbitals [such as $^1\Sigma_u^-$ ($\delta\delta$)] would be properly described.

D. Comparison with Observed Spectra. The states discussed in this study all occur in a region of energy that has not, to date, been examined experimentally for Ni_2. It is possible, however, to use information obtained here concerning the ground state to comment on recently observed ultraviolet–visible spectra for the dimer. The two most complete studies, those of Ozin[18] and Hulse and Moskovits,[19] were both obtained with Ni deposited in argon matrices and show good agreement in the observed bands. Both studies show well-resolved bands at approximately 2.4 and 3.5 eV with vibrational spacings of about 330 cm^{-1} (Ozin reports 360 cm^{-1} for the 2.4-eV band). A third structureless band is noted in both studies at around 2.9 eV.

An important feature in the well-resolved bands is that the measured vibrational frequencies are very close to the value of 344 cm^{-1} obtained here for the ground state. Electronic transitions of the form $\sigma_{4s} \rightarrow \pi_{4p}$ or $\sigma_{4s} \rightarrow \sigma_{4s}^*$ that would be expected to carry oscillator strength should also lead to significant changes in vibrational frequency and thus do not represent reasonable assignments for these transitions. Similar arguments apply to allowed 3d $\rightarrow \sigma_{4s}^*$ transitions (since this produces a more weakly bound $4s^3$ bonding configuration). On the other hand, transitions of the form 3d $\rightarrow \pi_{4p}$ should have little effect upon the vibrational frequency and represent the most likely assignments for these transitions. In the separate atom, the analogous 3d $\rightarrow$ 4p transitions occur in the range from about 3.2 to 5.8 eV.[4] Upon formation of Ni_2, the 3d levels are only weakly perturbed, whereas the 4pπ level is stabilized through formation of the partial π bond. As a result, the molecular 3d $\rightarrow \pi_{4p}$ transition energy should be reduced somewhat (~0.5 eV) relative to the atomic analogue, which is consistent with the observed bands.

Hulse and Moskovits,[19] through comparison with published Xα and extended Hückel treatments of Ni_2, reach similar conclusions regarding the origin of the two structured bands. The third band, owing to its structureless nature, apparently involves significant geometry change and thus weakening of the Ni_2 bond. For these reasons, Hulse and Moskovits assign this band to the $\sigma_{4s} \rightarrow \sigma_{4s}^*$ transition, expected to be strong. Though we cannot rule out such an assignment, simple overlap arguments suggest that this transition should occur at much higher energy. For clarity, we will consider the forbidden σ_{4s}

Table IV. Total Energies[a] for Some of the Low-Lying States of Ni_2 and Ni_2^+ from GVB-CI and POL-CI Calculations at R = 2.01 Å (Energies in hartrees)

	Ni_2				Ni_2^+	
state	$^1\Gamma_g(\delta\delta)$	$^3\Sigma_g^-(\delta\delta)$	$^3\Gamma_u(\delta\delta)$	$^1\Sigma_g^+(\sigma\sigma)$	$^4\Sigma_u^-(\delta\delta)$	$^2\Sigma_g^+(\sigma\sigma)$
GVB-CI	−81.0870	−81.0867	−81.0864	−81.0563	−80.7729	−80.7211
POL-CI	−81.0960	−81.0956	−81.0943	−81.0721	−80.8595	−80.8037

[a] Using the effective potential, atomic energies are Ni (^{3}D) = −40.4943 and Ni^+ (^{2}D) = −40.2150 hartrees.

Table V. Effects of Spin-Orbit Coupling on Lowest Ni_2 States

state	Ω[a]	$\hat{H}_0$, eV[b]	$\hat{H}_0 + \hat{H}_{SO}$[c]	dominant admixture due to spin-orbit coupling	
$^1\Sigma_g^+(\delta\delta)$	0	0.00	−0.147	$^3\Sigma_g^-(\delta\delta)$	(50%)
$^1\Gamma_g(\delta\delta)$	4	0.001	−0.030	$^3\Phi_{u_4}(\pi\delta)$	(10%)
$^1\Sigma_u^-(\delta\delta)$	0	0.006	−0.140	$^3\Sigma_u^-(\delta\delta)$	(50%)
$^3\Sigma_g^-(\delta\delta)$	1	0.009	−0.020		
	0	0.009	−0.098	$^1\Sigma_g^+(\delta\delta)$	(50%)
$^3\Sigma_u^+(\delta\delta)$	1	0.016	−0.009		
	0	0.016	0.115	$^1\Sigma_u^-(\delta\delta)$	(50%)
$^3\Gamma_u(\delta\delta)$	5	0.016	−0.135		
	4	0.016	−0.008		
	3	0.016	0.135		

[a] Total angular momentum about axis. [b] From GVB-CI calculations. [c] Rediagonalized from 100 × 100 matrix.

→ σ_{4s}* singlet-triplet transition which must, by Hund's rule, occur at lower energies than the allowed singlet-singlet transition. Ignoring all but the 4s electrons, this leads to an excited-state wave function of

$$\phi_{4s}{}^* = \mathcal{A}\{(\sigma_{4s_g}\sigma_{4s_u} - \sigma_{4s_u}\sigma_{4s_g})(\alpha\alpha)\} = \mathcal{A}\{(\ell r - r\ell)(\alpha\alpha)\}$$

where the equivalent valence bond wave function is also shown. Evaluating the energy for this wave function using the approach shown in Appendix I leads to an expression

$$E_{4s}{}^* = E_{c\ell} - \frac{2S\tau_1}{1 - S^2}$$

which is very similar (the reason for choosing the triplet state) in form to that given in the Appendix for the ground state,

$$E_{g.s.} = E_{c\ell} + \frac{2S\tau_1}{1 + S^2}$$

For bond lengths near the minimum $S \approx 0.7$ leading to

$$E_{4s}{}^* = E_{c\ell} - 2.75\tau_1$$

$$E_{g.s.} = E_{c\ell} + 0.94\tau_1$$

For all values of R, τ_1 is negative and dominates $E_{c\ell}$. Thus, near the minimum where the ground state is bound by 2.9 eV, the excited triplet state should be almost 8 eV higher by this simple approach (assuming $|\tau_1| \gg E_{c\ell}$). Using this value as a lower bound for the allowed singlet-singlet transition suggests that the 2.9 eV observed band must have a different source. The most reasonable transition still consistent with the changes implied by the spectra is a $\sigma_{4s} \rightarrow \pi_{4p}$. Analogous atomic transitions occur in the region of 3.5-3.7 eV,[4] which is more consistent with the observed band position. Clearly these bands require further study, and a more quantitative analysis will be presented from this laboratory at a later date.

E. Bond Energies. Beyond these spectroscopic studies, there is little detailed experimental information regarding Ni_2. Bond energies have been estimated by Kant[1] using mass spectroscopic data. Assuming values for bond length, vibrational frequency, and degeneracy, he obtains $D_e(Ni_2)$ = 2.4 ± 0.2 eV and $D_e(Ni_2^+)$ = 3.8 ± 0.2 eV. This compares with $D_e(Ni_2)$ = 2.9 eV and $D_e(Ni_2^+)$ = 4.1 eV from our calculations. The experimental estimate changes very little (~0.1 eV) upon incorporating our calculated molecular constants into the formula used by Kant.

F. Spin-Orbit Coupling. As the spectrum of states found in this study spans a very narrow energy range, the possible influence of spin-orbit coupling on the ordering of states merits some consideration. A very simple assessment of the importance of this effect is made possible by the fact that each of the states involves highly localized singly occupied 3d orbitals. Our approach was as follows. We considered the 100 lowest states $\{\psi_i = 1, 2, \ldots, 100\}$ corresponding qualitatively to a d^9 configuration on each of the two Ni atoms. The eigenvalues $\{E_i{}^0, i = 1, 2, \ldots, 100\}$ illustrated in Figure 1 correspond to diagonalizing the usual nonrelativistic Hamiltonian over these 100 states. Considering the simplified spin-orbital Hamiltonians

$$\mathcal{H}_{SO} = \sum_j \zeta_j(r_j)\hat{\ell}_j\hat{s}_j$$

we evaluated the 100 × 100 matrix

$$\langle 4_i|(\mathcal{H}_0 + \mathcal{H}_{SO})|\psi_j\rangle = E_i{}^0\delta_{ij} + \langle\psi_i|\mathcal{H}_{SO}|\psi_j\rangle$$

and diagonalized this matrix to allow opponent spin-orbital eigenstates. In the process of evaluating $\langle\psi_i|\mathcal{H}_{SO}|\psi_j\rangle$ we made the additional simplifications of (1) ignoring the very slight contamination of pπ character into the dπ orbitals, (2) the slight mixing of pσ and s character with the dσ orbitals, (3) including only the one center contributions to $\mathcal{H}_{SO}$, and (4) ignoring the overlap of d orbital on different centers (the actual overlaps ranged from 0.006 au for dδ to 0.04 and 0.06 for dπ and dσ, respectively). In addition we set the radial integrals $\langle\phi_d|\zeta(r)|\phi_d\rangle$ to −0.0756 eV, obtained from a fit to the spin-orbit splittings observed for the ^{3}D state of the Ni atom.[4]

The resulting ordering of the eigenstates including spin-orbit coupling differs very little from the scheme presented in Figure 1. Table V shows the energies with and without spin-orbital coupling for the lower states. The preference for δ holes rather than π or σ in the lowest states is not disturbed. Since the $\zeta(r)$ prefactor in each of the one-electron matrix elements is negative, the greatest stabilization due to spin-orbit effects occurs for spin orbitals of maximum total angular momentum about the axis, Ω. Thus the $^3\Gamma_{u_5}$ state which appears, using complex orbitals, as

$$^3\Gamma_{u_5} = \mathcal{A}\{\delta_\ell{}^{2+}\delta_r{}^{2+}\alpha\alpha\}$$

shows the strongest stabilization. Similarly, the $^3\Gamma_{u_3}$ state

$$^3\Gamma_{u_3} = \mathcal{A}\{\delta_\ell{}^{2+}\delta_r{}^{2+}\beta\beta\}$$

experiences the strongest destabilization. The lowest state, including spin-orbit coupling, is

$$^1\Sigma_g^+(\delta\delta) + {}^3\Sigma_g^-(\delta\delta)$$

with the state

$$^1\Sigma_u^-(\delta\delta) + {}^3\Sigma_u^+(\delta\delta)$$

only 0.007 eV higher. The $^3\Gamma_{u_5}$ state lies 0.012 eV above the ground state. Such small splittings among the lowest states could be perturbed by other weak interactions.

Acknowledgments. This work was supported in part by a grant (DMR74-04965) from the National Science Foundation. Acknowledgment is made to the donors of the Petroleum Research Fund, administered by the American Chemical Society, for partial support of this research. We thank Dr. Carl Melius for helpful discussions.

Appendix I

Through the use of valence bond wave functions it is possible to make a direct comparison between the energy expressions arising from one- and two-electron bonds. For the one-electron bond, a simple wave function may be assumed,

$$\varphi_1 = \{(\ell + \mathrm{r})\alpha\} \tag{A-1}$$

and for the two-electron bond,

$$\varphi_2 = \mathcal{A}\{(\ell\mathrm{r} + \mathrm{r}\ell)(\alpha\beta - \beta\alpha)\} \tag{A-2}$$

These give rise to the energy expressions

$$E_1 = \frac{\langle\varphi_1|\mathcal{H}|\varphi_1\rangle}{\langle\varphi_1|\varphi_1\rangle} = \frac{h_{\ell\ell} + h_{\ell\mathrm{r}}}{1+S} + \frac{1}{R}$$

$$E_2 = \frac{\langle\varphi_2|\mathcal{H}|\varphi_2\rangle}{\langle\varphi_2|\varphi_2\rangle} = \frac{2h_{\ell\ell} + 2Sh_{\ell\mathrm{r}} + J_{\ell\mathrm{r}} + K_{\ell\mathrm{r}}}{1+S^2} + \frac{1}{R} \tag{A-3}$$

where the terms have their usual meaning.

Partitioning the energy expression into classical terms[20] [arising from ℓ in (A-1) or $\ell\mathrm{r}$ in (A-2)] and the exchange terms [arising from the superposition of terms in (A-1) or (A-2)] leads to

$$E_1 = E_1^{c\ell} + E_1^{\mathrm{x}} \qquad E_2 = E_2^{c\ell} + E_2^{\mathrm{x}} \tag{A-4}$$

where

$$E_1^{c\ell} = \tfrac{1}{2}(h_{\ell\ell} + h_{\mathrm{rr}}) + 1/R$$

$$E_2^{c\ell} = h_{\ell\ell} + h_{\mathrm{rr}} + J_{\ell\mathrm{r}} + 1/R$$

$$E_1^{\mathrm{x}} = \frac{\epsilon_1 - SE_1^{c\ell}}{1+S} = \frac{\tau_1}{1+S}$$

and

$$E_2^{\mathrm{x}} = \frac{\epsilon_2 - S^2E_2^{c\ell}}{1+S^2} = \frac{2S\tau_1 + \tau_2}{1+S^2}$$

where

$$\tau_1 \equiv h_{\ell\mathrm{r}} - Sh_{\ell\ell} \text{ and } \tau_2 \equiv K_{\ell\mathrm{r}} - S^2J_{\ell\mathrm{r}}$$

and where the exchange terms dominate the bonding. The term τ_2 is positive but dominated by τ_1 which is negative. Neglecting τ_2 we can write

$$E_1^{\mathrm{x}} = \frac{\tau_1}{1+S}$$

and

$$E_2^{\mathrm{x}} = \frac{2S\tau_1}{1+S^2}$$

Thus the relative strengths of the one- and two-electron bonds depend upon the overlap. The exchange terms are equal for $S = 0.42$. Thus for this value of the atomic orbital overlap, the one- and two-electron bonds will be almost equal in strength. For smaller overlap (longer bond length), the one-electron bond will be stronger.

References and Notes

(1) A. Kant, *J. Chem. Phys.*, **41**, 1872 (1964).
(2) (a) A. Kant, *J. Chem. Phys.*, **41**, 3806 (1964); (b) P. Schissel, *Ibid.*, **26**, 1276 (1957); (c) K. A. Gingerich, *J. Cryst. Growth*, **9**, 31 (1971); (d) R. Busby, W. Klotzbücher, and G. A. Ozin, *J. Am. Chem. Soc.*, **98**, 4013 (1976).
(3) T. C. DeVore, A. Ewing, H. F. Franzen, and V. Calder, *Chem. Phys. Lett.*, **35**, 78 (1975).
(4) C. E. Moore, "Atomic Energy Levels", Vol. II, National Bureau of Standards, Washington, D.C., 1949.
(5) S. P. Walch and W. A. Goddard III, *J. Am. Chem. Soc.*, **98**, 7908 (1976).
(6) δ_1 refers to $\delta_{x^2-y^2}$ and δ_2 to δ_{xy}.
(7) This assumption is based on arguments given in section IIA regarding hybridization of the 4s orbital in Ni_2. With ionization from the σ shell, hybridization requires mixing of low-lying s^0d^9 configurations of Ni^+. Removing a $3d_\pi$ or $3d_\delta$ electron necessitates mixing of very high-lying s^2d^7 configurations to hybridize the 4s orbital. Alternatively, an examination of orbital energies for Ni_2 shows the $3d_\sigma$ combination electrons to be least bound.
(8) See, for example, L. R. Kahn and W. A. Goddard III, *J. Chem. Phys.*, **56**, 2685 (1972).
(9) C. F. Melius, B. D. Olafson, and W. A. Goddard III, *Chem. Phys. Lett.*, **28**, 457 (1974).
(10) M. Sollenberger, C. F. Melius, and W. A. Goddard III, to be published; see also M. Sollenberger, M.S. Thesis, California Institute of Technology, 1976.
(11) A. J. H. Wachters, *J. Chem. Phys.*, **52**, 1033 (1970).
(12) W. B. Pearson, "A Handbook of Lattice Spacings and Structures of Metals and Alloys", Pergamon Press, Elmsford, N.Y., 1958.
(13) F. A. Cotton and G. Wilkinson, "Advanced Inorganic Chemistry", Interscience, New York, N.Y., 1972.
(14) Yu. M. Efremov, A. N. Samoilova, and L. V. Gurvich, *Opt. Spektrosk.*, **36**, 381 (1974).
(15) E. P. Kundig, M. Moskovits, and G. A. Ozin, *Nature (London)*, **254**, 503 (1975).
(16) T. H. Upton, C. F. Melius, and W. A. Goddard III, to be submitted.
(17) G. Herzberg, "Spectra of Diatomic Molecules", Van Nostrand-Reinhold, Princeton, N.J., 1950.
(18) G. A. Ozin, private communication.
(19) M. Moskovits and J. E. Hulse, *J. Chem. Phys.*, **66**, 3988 (1977), and references cited therein.
(20) C. W. Wilson, Jr., and W. A. Goddard III, *Theor. Chim. Acta*, **26**, 195 (1972).